Polymer 155 (2018) 58–63

Contents lists available at ScienceDirect

Polymer

journal homepage: www.elsevier.com/locate/polymer

Nafion membrane channel structure studied by small-angle X-ray scattering and Monte Carlo simulations

S.P. Fernandez Bordín[a], H.E. Andrada[a], A.C. Carreras[a], G.E. Castellano[a,*], R.G. Oliveira[b], V.M. Galván Josa[a]

[a] Universidad Nacional de Córdoba, Facultad de Matemática, Astronomía, Física y Computación, Instituto de Física Enrique Gaviola (IFEG), CONICET, Medina Allende s/n, Ciudad Universitaria (5000), Córdoba, Argentina

[b] Universidad Nacional de Córdoba, Facultad de Ciencias Químicas, Departamento de Química Biológica Ranwell Caputto, Centro de Investigaciones en Química Biológica de Córdoba (CIQUIBIC), CONICET, Haya de la Torre s/n, Ciudad Universitaria (5000), Córdoba, Argentina

HIGHLIGHTS

- Nafion 117 membrane structure was studied through SAXS pattern simulations.
- Measurements were taken for different moisture conditions and for different temperatures.
- A simulation program was developed to produce SAXS profiles for the structure model proposed.
- Suitable electron density maps were obtained, based on a core-shell type channel structure.

ARTICLE INFO

Keywords:
Nafion membrane
SAXS
Water channel
Inverse core-shell structure

ABSTRACT

The structure of Nafion 117 membranes was studied through SAXS experiments and 2D pattern simulations. Measurements were taken for different moisture conditions by synchrotron radiation, and for different temperatures through X-ray tube irradiation. The experimental profiles were fitted through simulations based on a new structural model including: the amorphous polymer matrix, polymer crystallites, and inverse core-shell type channels conformed by water cylinders and sulfonic chains. The geometrical parameters intervening in the simulation of the SAXS patterns were optimized for each experimental condition. This approach allowed the proper description of the experimental SAXS profiles for the various moisture conditions studied. In addition, a recent lamelar model was also included in the assessments, and the corresponding performances were discussed.

1. Introduction

The polymer electrolyte membrane fuel cell (PEMFC) has become a promising type of fuel cell as a clean energy source. The membrane used as electrolyte is a key component in PEMFCs, and it must have a high proton conductivity, low electron conductivity, low fuel permeability, good chemical and thermal stability, and good mechanical properties. One of the most common and commercially available fuel cell electrolytes is the Nafion® membrane, manufactured by DuPont.

Nafion is a copolymer of tetrafluoroethylene (PTFE) and a vinyl ether containing a sulfonyl fluoride group at the end. It has received a considerable attention as a proton conductor for PEMFCs due to its excellent thermal and mechanical properties [1,2].

The morphology of Nafion membranes is a subject of continuous research due to its strong influence on their properties. The mechanical, thermal, and oxidative stability of the Nafion membrane is directly related with its polymer structure, although the relationship between its nanostructure and proton conductivity is still not clear.

The first approach for Nafion structure, called the cluster-channel or cluster-network model, consisted of a distribution of 4 nm sulfonate ion clusters held within a continuous fluorocarbon lattice. Narrow water channels of about 1 nm in diameter interconnect the clusters, which explains the membrane transport properties [3–5].

Later structural investigations have yielded other ionic domain shapes, namely, a core-shell sphere model where the ion-rich core is surrounded by an ion poor shell; a rod model where the sulfonic groups arrange into crystal-like rods; and a more recent lamelar model proposed by Kreuer and Portale [6], which provides arguments supporting locally flat domains.

The various structural existent models involve an ionomer domain,

* Corresponding author.
E-mail address: gcas@famaf.unc.edu.ar (G.E. Castellano).

https://doi.org/10.1016/j.polymer.2018.09.014
Received 1 June 2018; Received in revised form 15 August 2018; Accepted 7 September 2018
Available online 15 September 2018
0032-3861/

a crystalline component, an amorphous phase, and water; regardless the possible variations, all of them produce appropriate raw descriptions of the membrane structure [7]. The differences rely in the distribution of each of these phases.

The performance of many of these models has been surveyed by small-angle X-ray scattering (SAXS) or neutron scatering (SANS), as that proposed by Schmidt-Rohr and Chen [8], in which the Nafion structure is described with cylindrical water channels and PTFE crystallites within the non-crystalline PTFE matrix. The SAXS/SANS profile $I(q)$ of a Nafion membrane has two main features: the ionomer peak at $q \approx 1.57\,\mathrm{nm}^{-1}$, and the matrix knee at $q < 0.7\,\mathrm{nm}^{-1}$. The ionomer peak is produced by the membrane water channel periodicity within the clusters. The width of the peak is related to structural disorder in the clustering of water domains [6,8], and the position is associated to the hydration degree [6,8–10]. The matrix knee is caused by the fluorocarbon polymer crystallites randomly distributed in the amorphous polymer matrix, and its intensity depends on the degree of crystallinity [11]. These crystallites are an important component of Nafion membranes, since they give them specific mechanical properties [12].

In this work, the Nafion membrane channel structure was studied by means of SAXS. Experimental SAXS patterns acquired by synchrotron radiation and by a conventional X-ray source were fitted by optimizing a parallel inverse core-shell cylinder structure obtained through Monte Carlo simulations. This approach is based on the Schmidt-Rohr and Chen [8] model, in which parallel cylindrical water channels (non-core-shell) and polymer crystallites are distributed within an amorphous polymer matrix. The reasons supporting this choice are that this approach easily describes the hydrophilic (SO_3 groups and water) and hydrophobic (fluorocarbon chain, CF_2) domains, accounting for many of the physicochemical properties, such as proton conductivity, ion exchange capacity and water absorption capacity. The main improvement introduced here is the difference in electron density between the sulfonic chains of the Nafion structure and the amorphous polymer matrix. As a consequence, an improved electron density map was obtained, following the hexagonal structure reported by Lyonnard et al. [13].

Hexagonal-like cylindrical inverse core-shell water channels were generated by Monte Carlo simulations, and the membrane structure was furnished by the aggregation of these clusters through random walks. The electron density maps used to provide the simulated SAXS intensity profiles were generated with these water channels along with prismatic polymer crystals dispersed in the amorphous polymer matrix. The final Nafion membrane structure was obtained by optimizing the parameters involved, to achieve the best match to the experimental profiles. It is important to stress that variations in the membrane structure due to changes in the environmental conditions (e.g., pressure, pH, temperature or moisture) may be readily assessed through this approach, since the simulated SAXS/SANS patterns can be computed easily. In order to check the self consistency of the present approach, the SAXS patterns corresponding to different temperature and moisture conditions were successfully reproduced. In addition, ionic flat domains [6] were also implemented in the simulations, with the aim of comparing the performances of the different models.

2. Experiment

A commercial Nafion 117 polymeric membrane (Dupont) 183 μm thick was chosen for the present study. Before the SAXS measurements, Nafion samples ($\sim 1\,\mathrm{cm}^2$) were subjected to the activation treatment suggested in Ref. [14], intended to protonate the sulfonic groups, which are the membrane active sites:

- heating in Milli-Q water up to 80°C, and keep this temperature for 1 h;
- rinsing with Milli-Q water;
- heating in hydrogen peroxide 3% solution up to 80°C, and keep this temperature for 1 h;
- rinsing with Milli-Q water;
- heating in a 0.5 M H_2SO_4 solution up to 80°C, and keep this temperature for 1 h;
- rinsing with Milli-Q water;
- keep under water.

SAXS measurements were performed at the SAXS1 beamline of the Brazilian Synchrotron Light Laboratory (LNLS, Brazil), in transmission mode. The selected beam energy was 8 keV, with a beam size of $1.5 \times 0.5\,\mathrm{mm}^2$. Data were collected with a two-dimensional Pilatus 300 K (Dectris) detector, background corresponding to the dark noise and the empty cell signal being subtracted. Each SAXS pattern was acquired in a q-range $0.12\,\mathrm{nm} \leq -1\, q \leq 4.58\,\mathrm{nm}^{-1}$ at constant temperature (25°C) and moisture conditions, the counting time being 10 s in all cases. The first measurement was acquired at 100% moisture, and this was slowly reduced between measurements, down to 50% ambient moisture; 24 h were allowed before taking the last measurement, in order to ensure room conditions (RH 50%). On the other hand, the simulation program developed along this work was used also to provide information about the evolution of the membrane structure when heating the sample at RH 50%. To this aim, SAXS profiles at different temperatures were acquired in a motorized Xeuss 1.0 equipment (Xenocs) with a Pilatus 100 K (Dectris) detector. The selected beam energy was 8 keV, with a beam size of $0.5 \times 0.5\,\mathrm{mm}^2$, q values ranging from $0.1\,\mathrm{nm}^{-1}$–$2.5\,\mathrm{nm}^{-1}$. Since the beam flux is quite lower in this case, samples were irradiated during 300 s. A Linkam® HFSX350 heating and freezing stage was used in order to program the sequential temperatures imposed to the sample.

In order to assess changes in the sample crystallinity due to the activation treatment, X-ray diffraction (XRD) patterns were acquired in an PANalytical Empyrean diffractometer with a copper tube and a graphite monochromator at 40 keV and 40 mA, 0.1° step size and the effective counting time was 100 s/step.

3. Methods

In the model presented here, electron density maps were furnished by Monte Carlo simulation where inverse core-shell like cylindrical water channels are thus packed in an inverted micellar configuration, assigning different electron densities to the water channel cores, the sulfonic shells, the dispersed polymer crystallites, and the amorphous polymer matrix. The electron densities used were $0.548\,e/\text{Å}^3$ for the amorphous polymer matrix, $0.632\,e/\text{Å}^3$ for the polymer crystallites, 0.557–0.589 $e/\text{Å}^3$ for the sulfonic chain and $0.334\,e/\text{Å}^3$ for the water channels [15,16].

Fig. 1 shows a typical cluster produced by the simulation algorithm developed. Such clusters are built up with seven channels in a hexagonal array, six located in the hexagon vertices and one at its center. The procedure to generate a cluster was: firstly, the channel core radii were sampled from the distribution proposed by Schmidt-Rohr and Chen [8], setting the center r of this distribution according to the membrane hydration degree. A shell 0.7–1 nm thick (uniform random distribution) was then added to each channel corresponding to the sulfonic chains. Channels were generated sequentially, in the order shown in Fig. 1. The location of each vertex channel center was chosen by adding a random two-dimensional Gaussian perturbation to the positions of the vertices of a regular hexagon, with a standard deviation $\sigma = \langle v \rangle/3$, where the fitting parameter $\langle v \rangle$ is a measure for the structure disorder; this perturbation was constrained to avoid the overlapping of water channels. The interplanar distance d_{10} responsible for the appearance of the ionomer peak is associated to the hexagon apothem.

To locate the clusters in the matrix, a Diffusion Limited Cluster Aggregation (DLCA) model was used. In this model, a seed cluster is

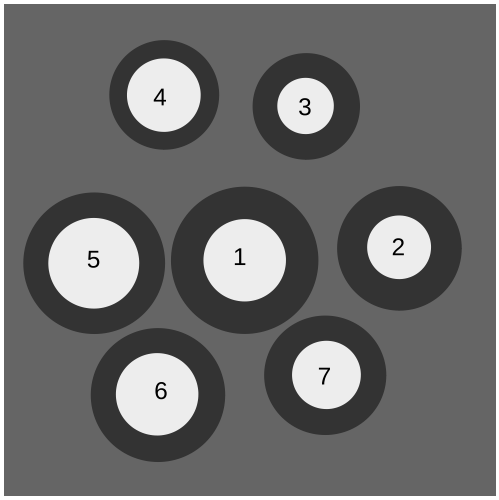

Fig. 1. Scheme of a finished hexagonal cluster. The numbers indicate the sequential generating order.

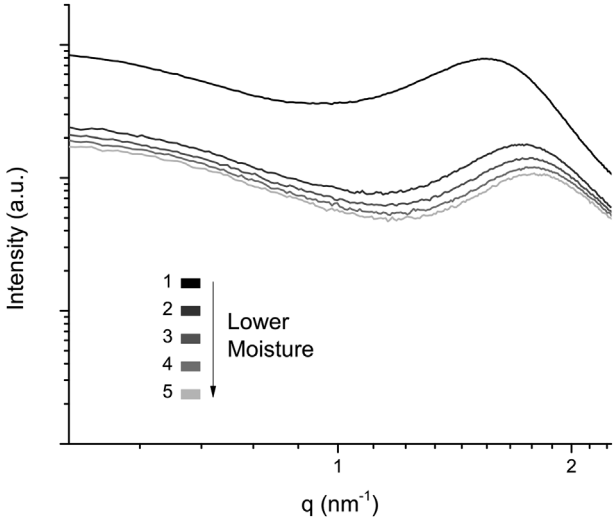

Fig. 2. SAXS profiles measured for the Nafion membrane with different hydration conditions.

placed in the middle of the map, and then the rest of the clusters are generated over a circumference. Then the clusters perform a random walk approaching the center, and stick to the cluster aggregate when they get in contact.

Once the cluster aggregate is complete, polymer crystallites are added. These crystallites were modeled as rectangular transversal sections, according to Schmidt-Rohr and Chen [8], Van der Heijden et al. [17] and Kim et al. [18], with one side ranging between 1.5 and 3 nm, and the second between 1.5 and 5.5 nm, their ratios running from 1/1 to 1/1.8. The crystals were located in a random way over the polymer amorphous matrix, following a 2D uniform distribution.

With the density maps built up as described, SAXS profiles were simulated using the algorithm proposed by Schmidt-Rohr [15], which allows to model the scattering intensity as a function of q, $I(q)$, by using the Inverse Fourier Transform in a two-dimensional electron density map for long parallel structures. For each measured spectrum, the parameters r, d_{10} and $\langle v \rangle$, as well as the polymer crystallite sizes and number, were fitted in order to achieve the best description of the experimental data, fixing the electron densities over temperature and moisture changes. In other words, only structural parameters were allowed to vary.

With the aim of implementing this methodology in a recent structural model, the lamelar structure suggested in Ref. [6] was also simulated following a procedure similar to that described above. In this case, the adjustable parameters are the structural correlation length $d_p + d_w$, where p and w stand for polymer and water layer respectively along the stacking direction; the mean square fluctuation of the distance between water layers Δ describing the stacking disorder; and the mean number of stacks N. The routine developed permits to include tortuosities in the flat interfaces, which enabled to furnish SAXS patterns corresponding to perfectly flat domains along lateral lengths not greater than $\sim$ 4 nm [6].

4. Results and discussion

Fig. 2 displays the experimental SAXS profiles for the Nafion membrane in five different moisture conditions, starting from a hydrated state similar to the moisture degree at which the membrane operates in a fuel cell (curve 1), until it reaches a stationary moisture equilibrium at laboratory conditions (curve 5). In these curves, the ionomer peak and the matrix knee are clearly present. The ionomer peak corresponds to the first maximum in the structure factor [19], which evidences a local ordering within the ionic clusters [20]. The matrix knee is usually attributed to a supralamellar distance in the crystalline part on the polymer and its intensity depends on the degree of crystallinity [11].

With the aim of modeling the Nafion channel structure, electron density maps were furnished for locally flat and hexagonal domains, following the procedure described in the previous section. As an example, Fig. 3 displays the density maps obtained for the present inverse core-shell model corresponding to the maximum moisture degree considered in this work. The SAXS profiles resulting from these maps were fitted to the experimental data. Fig. 4 shows a comparison between measured and simulated profiles corresponding to two different hydration conditions (curves 1 and 5 in Fig. 2). As expected, the ionomer peak is readily reproduced with an appropriate correlation length characterizing a determined structure. For the lamelar structure, it corresponds to the length embracing two contiguous water-polymer layers ($d_p + d_w$); whereas for the locally hexagonal structure, this

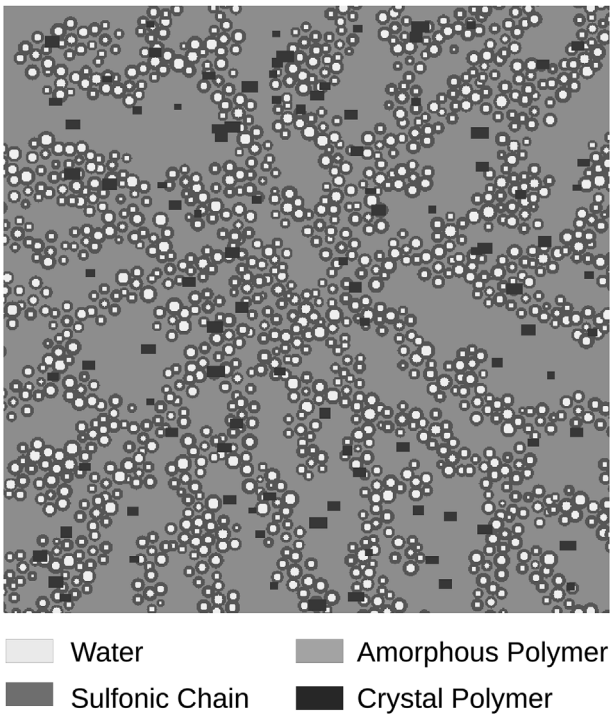

Fig. 3. Simulated electron density map for the maximum hydration condition.

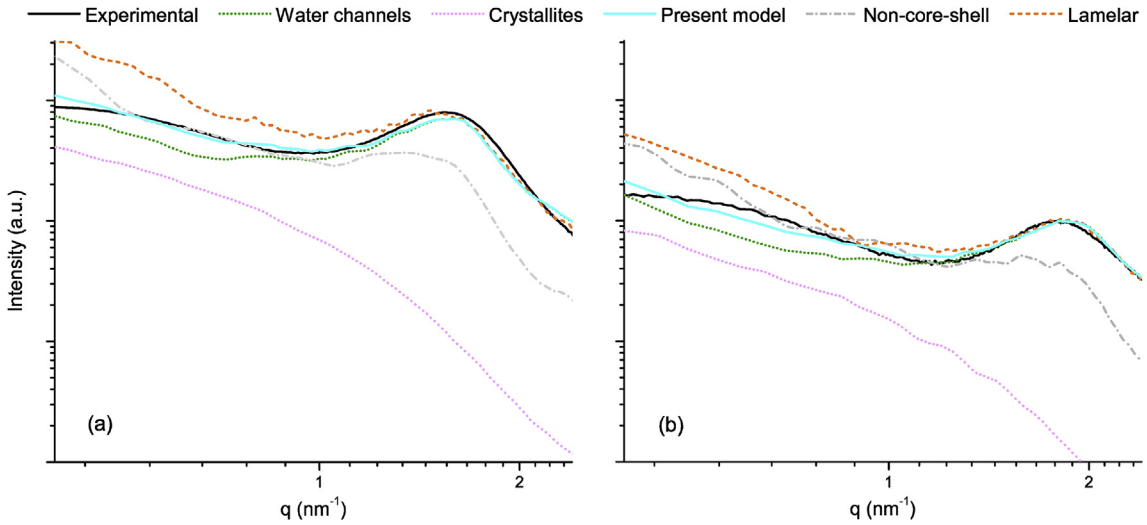

Fig. 4. Experimental and simulated SAXS profiles. Different components for curve 1 (a), and curve 5 (b) from Fig. 2.

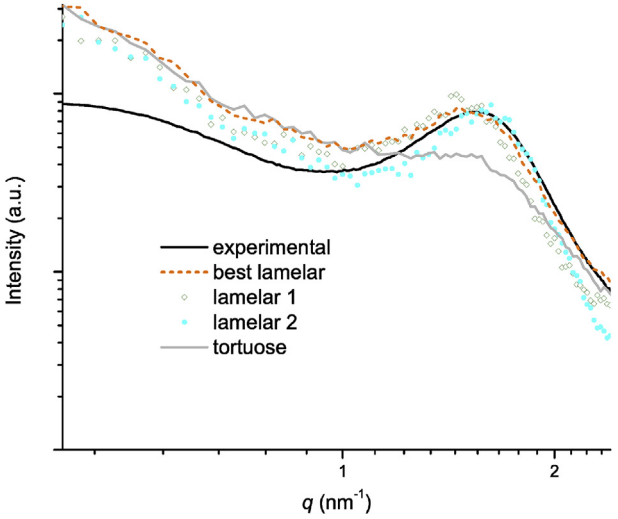

Fig. 5. Experimental SAXS profiles and those simulated for the lamelar model with different parameters. Best lamelar fit (no roughness, shown in Fig. 4): $d_p + d_w = 3.85$ nm, $\Delta = 1.8$ nm; lamelar 1: no roughness, $d_p + d_w = 4.00$ nm, $\Delta = 1.7$ nm; lamelar 2: no roughness, $d_p + d_w = 3.80$ nm, $\Delta = 1.4$ nm; tortuose: best configuration including roughness in the interfaces.

length is associated to the hexagon apothem (d_{10}). The matrix knee at lower q accounts for the polymer crystals, as previously established in the literature [8,21]. The predicted intensity for the low-q region is overestimated with the lamelar structure, even for different choices of the disorder in layer separation Δ. It is worth emphasizing that this overestimation would be even greater if the crystallite contribution is added (as discussed below). This discrepancy has been explained in Ref. [6] suggesting that "the structures are close to planar on a local scale only (≤ 4 nm), with tortuosities on longer scales". However, this artificial intensity increase for low q values is present even when taking roughness into account, as shown in Fig. 5; the effect of tortuosities manifests in a correlation loss which markedly reduces the ionomer peak (and eventually broadens it). Fig. 5 also includes lamelar SAXS patterns corresponding to different parameter settings.

In order to compare the present inverse core-shell model with the parallel cylindrical non-core-shell approach, Monte Carlo simulations for electron density maps were also furnished for this latter, following the procedure described above with no distinction between sulfonic chains and amorphous polymer. Fig. 4 shows that the non-core-shell model adequately describes the experimental data for low q values, since both models share the crystallite phase; however, for q values around the ionomer peak, this description markedly underestimates the measured intensity.

As mentioned above, crystallites are an important component of the structure of Nafion membranes. Schmidt-Rohr and Chen [8] show, in accordance with other authors [12,16,18], that polymer crystals are responsible for approximately 3/4 of low q scattering intensity. In the present simulations, crystals were considered as extended rectangular prisms of $\sim 8\,\mathrm{nm}^2$ average cross sections. The volume fraction of crystallites produced by the simulations ranged between 1 and 2%, lesser than the results obtained by Schmidt-Rohr and Chen [8] and Knox et al. [21], who estimated values between 8 and 10%. These differences may be due to the activation treatment carried out, which could alter the membrane crystallinity. In order to check this issue, X-ray diffraction (XRD) measurements were performed in a Nafion membrane before and after the activation treatment. Fig. 6 shows examples for the XRD patterns acquired, along with fits to the first two-peak structure corresponding to an amorphous peak at $q = 11.64\,\mathrm{nm}^{-1}$ overlapping with a crystalline peak at $q = 12.34\,\mathrm{nm}^{-1}$, before and after treatment. The patterns also bear a less studied third peak at $q = 27.5\,\mathrm{nm}^{-1}$, whose corresponding Bragg distance (2.28 Å) might be interpreted as an intrachain distance within a Nafion chain [17,20,22]. A measure for the crystallinity can be assessed by integrating the crystalline intensity $I_c(q)$ and the total intensity $I_T(q)$ [17].

$$\chi_c = \frac{\int q^2 I_c(q)\, dq}{\int q^2 I_T(q)\, dq}\,.$$

In the present case, χ_c resulted in 0.177 for the untreated membrane, and 0.154 for the activated one, evidencing a loss of crystallinity with the activation process. This was to be expected, since the acid treatment produces partial polymer hydrolisis, as shown in Ref. [24]; this ensures a better interconnection of the hydrophillic channels, improving the proton conductivity. This reduction in χ_c is in agreement with the smaller volume fraction of the crystalline phase resulting from the present simulations, as discussed above.

Table 1 displays the results for the ionomer peak centroid q_p, the equivalent mean distance d_{10} in real space, and the full width at half maximum (FWHM) for the SAXS curves displayed in Fig. 2. In order to achieve an optimal description of the experimental SAXS profiles, the radial distribution proposed by Schmidt-Rohr [15] was modified for the present simulations by varying the r value and the corresponding radius range, according to the hydration degree: radii ranged between 0.55 and 1.45 nm with an average radius of 0.9 nm for curve 5, and between

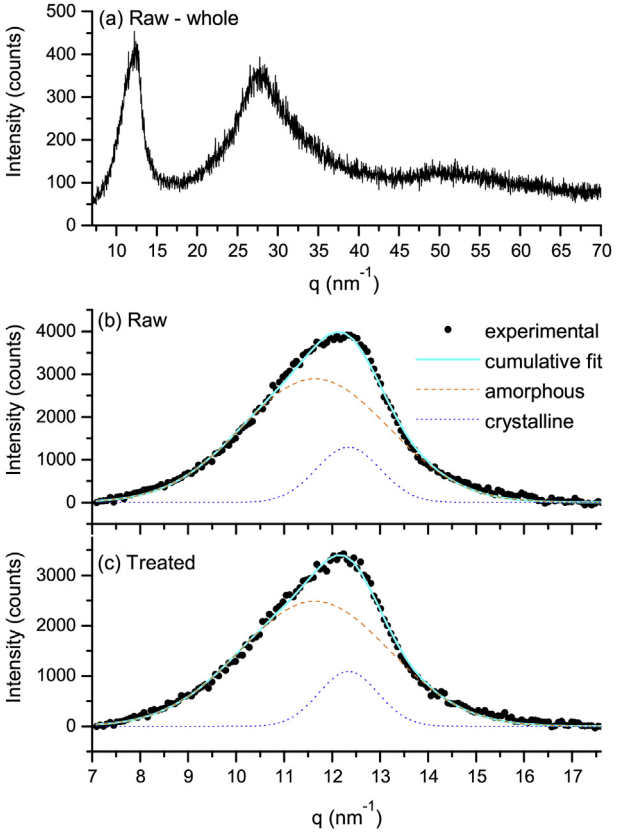

Fig. 6. X-ray diffraction patterns taken from the Nafion membrane: whole pattern before the activation treatment (a), and fits corresponding to the first two-peak structure with an amorphous peak at $q = 11.64\,\mathrm{nm}^{-1}$ overlapping with a crystalline peak at $q = 12.34\,\mathrm{nm}^{-1}$ before (b) and after (c) treatment, after background subtraction.

Table 1
Ionomer peak centroid q_p, equivalent mean distance d_{10} in real space, full width at half maximum (FWHM), and coherence lengths ℓ for the SAXS curves displayed in Fig. 2.

Curve	q_p (nm^{-1})	d_{10} (nm)	FWHM (nm^{-1})	ℓ (nm)
1	1.53	4.10	0.648	8.73
2	1.73	3.63	0.536	10.55
3	1.75	3.59	0.536	10.55
4	1.78	3.53	0.530	10.67
5	1.79	3.51	0.528	10.71

0.85 and 1.75 nm with an average radius of 1.22 nm for maximum hydration (curve 1).

The SAXS ionomer peak position is related to the membrane hydration degree [6,9,10]. As can be seen, the peak position shifts to higher q values as the membrane dehydrates. The results reported by Perrin et al. [10] suggest relative moisture values between ~15% (curve 5) and ~85% (curve 1), which respectively translate in volume percentages of ~10% and ~25%, according to Kong and Schmidt-Rohr [25]. These values are in agreement with the water volume concentrations resulting from the present simulations, which were 11% and 17% for curves 5 and 1, respectively. Water volume fractions of 20 and 24% for ionomer peak positions around $q = 1.4\,\mathrm{nm}^{-1}$, were reported by Rubatat et al. [19] and Gierke et al. [11], which are in clear accordance with the trend found here.

The ionomer peak width is attributed to the structural disorder present in the formation of clusters [6]. As the membrane dehydrates, the FWHM value decreases due to a reordering of channels (see Table 1); these FWHM values are associated with the coherence length

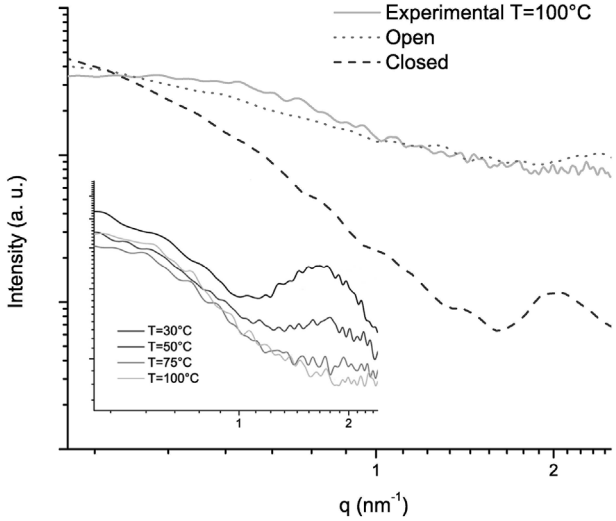

Fig. 7. SAXS profiles for the Nafion membrane when dehydrating at different temperatures. Continuous lines: experimental; dashed lines: simulated. Simulations account for the closed or open (hollow) channel approach (see text).

ℓ. In the simulations carried out here, the values obtained for the disordering parameter $\langle v \rangle$ were 2.4 and 2.1 nm for curves 1 and 5, respectively.

Fig. 7 shows the set of SAXS profiles measured at different temperatures and ambient moisture conditions. It can be seen that the ionomer peak shifts to higher q values as the temperature increases. This can be associated to a partial dehydration in the first stage of heating at 50°C. For a temperature of 100°C, water has evaporated almost completely.

In order to analyze the structure changes as the membrane dehydrates in these experiments, simulations were performed considering two possible models. In the first one, channels are expected to lose correlation lengths when temperature is raised and water is released: the membrane final structure is composed by the amorphous polymer matrix, the polymer crystallites and the disordered remainders of the water channels, constituted only by the sulfonic chains. The second approach maintains the structure of hexagonal clusters involving the inverse core-shell cylinders, where water is not present any more and their radii have been reduced but the hexagonal package remains (electron density zero). Fig. 7 shows a comparison of the experimental SAXS curve acquired at 100°C with the resulting profiles simulated through both models. As a result of the series of simulations carried out, for the model of channels closed after dehydration the final radial distribution ranged between 0.7 and 1.2 nm, with a mean value of 0.95 nm, and parameters $d_{10} = 2.4$ nm and $\langle v \rangle = 1$ nm. For the second approach of open (hollow) channels, the radial distribution ranged between 0.15 and 1.05 nm, with a mean value of 0.5 nm, $d_{10} = 2.5$ nm and $\langle v \rangle = 1$ nm. As can be seen in Fig. 7, the second model allows for a better description of the experimental SAXS profile, which suggests that channels remain open after dehydration.

5. Conclusions

The Nafion 117 membrane structure was characterized through SAXS measurements and Monte Carlo profile simulation. The experimental data taken for different moisture and temperature conditions, were compared with those simulated by means of a specific program developed to this aim, which provides suitable electron density maps, appropriately processed to produce simulated SAXS patterns, on the basis of an inverse core-shell type channel structure. The assessments included the parallel cylindrical non-core-shell [8] approach as well as

the recent lamelar structure model [6]. The improved electron density maps corresponding to parallel water cylindrical channels in the form of inverted micelles provide optimal fits to the experimental SAXS data.

The geometrical parameters involved in the electron density maps furnished for the simulation of the SAXS patterns were optimized for each experimental condition. The comparisons with the measured data allow to state that the inverse core-shell type channel model adequately describes the membrane structure for the various moisture conditions studied. As the membrane dehydrates, the results show that the water channel radii decrease, and the hexagonal cluster structure becomes more compact and ordered.

The simulation program developed was also used to study the channel structure as the membrane temperature increases at ambient moisture. The final profiles fitted suggest that channels do not collapse, but the structure of hexagonal clusters involving the core-shell cylinders is maintained after dehydration.

Acknowledgements

The authors are grateful to the Laboratório Nacional de Luz Síncrotron (LNLS) - SAXS1 beamline, Campinas, Brazil, and the Instituto de Investigaciones Fisicoquímicas Teóricas y Aplicadas (INIFTA), La Plata, Argentina, where the SAXS curves were taken.

References

[1] L. Boutsika, A. Enotiadis, I. Nicotera, C. Simari, G. Charalambopoulou, E. Giannelis, T. Steriotis, Nafion nanocomposite membranes with enhanced properties at high temperature and low humidity environments, Int. J. Hydrogen Energy 41 (2016) 22406–22414.
[2] L. Liu, W. Chen, Y. Li, An overview of the proton conductivity of Nafion membranes through a statistical analysis, J. Membr. Sci. 504 (2016) 1–9.
[3] W.Y. Hsu, T.D. Gierke, Ion transport and clustering in Nafion perfluorinated membranes, J. Membr. Sci. 13 (3) (1983) 307–326.
[4] C. Heitner-Wirguin, Recent advances in perfluorinated ionomer membranes: structure, properties and applications, J. Membr. Sci. 120 (1) (1996) 1–33.
[5] K.A. Mauritz, R.B. Moore, State of understanding of nafion, Chem. Rev. 104 (10) (2004) 4535–4586.
[6] K. Kreuer, G. Portale, A critical revision of the nano-morphology of proton conducting ionomers and polyelectrolytes for fuel cell applications, Adv. Funct. Mater. 23 (43) (2013) 5390–5397.
[7] J. Mališ, M. Paidar, T. Bystron, L. Brožová, A. Zhigunov, K. Bouzek, Changes in Nafion® 117 internal structure and related properties during exposure to elevated temperature and pressure in an aqueous environment, Electrochim. Acta 262 (2018) 264–275.
[8] K. Schmidt-Rohr, Q. Chen, Parallel cylindrical water nanochannels in Nafion fuel-cell membranes, Nat. Mater. 7 (1) (2008) 75–83.
[9] A. Rollet, G. Gebel, J.-P. Simonin, P. Turq, A SANS determination of the influence of external conditions on the nanostructure of Nafion membrane, J. Polym. Sci. B Polym. Phys. 39 (5) (2001) 548–558.
[10] J. Perrin, S. Lyonnard, F. Volino, Quasielastic neutron scattering study of water dynamics in hydrated Nafion membranes, J. Phys. Chem. C 111 (8) (2007) 3393–3404.
[11] T.D. Gierke, G.E. Munn, F. Wilson, The morphology in Nafion perfluorinated membrane products, as determined by wide- and small-angle x-ray studies, J. Polym. Sci. Polym. Phys. Ed 19 (11) (1981) 1687–1704.
[12] R.B. Moore III, C.R. Martin, Chemical and morphological properties of solution-cast perfluorosulfonate ionomers, Macromolecules 21 (5) (1988) 1334–1339.
[13] S. Lyonnard, Q. Berrod, B.-A. Brning, G. Gebel, A. Guillermo, H. Ftouni, J. Ollivier, B. Frick, Perfluorinated surfactants as model charged systems for understanding the effect of confinement on proton transport and water mobility in fuel cell membranes. A study by QENS, Eur. Phys. J. Spec. Top. 189 (1) (2010) 205–216.
[14] R. Kuwertz, C. Kirstein, T. Turek, U. Kunz, Influence of acid pretreatment on ionic conductivity of nafion membranes, J. Membr. Sci. 500 (2016) 225–235.
[15] K. Schmidt-Rohr, Simulation of small-angle scattering curves by numerical Fourier transformation, J. Appl. Crystallogr. 40 (1) (2007) 16–25.
[16] E.J. Roche, M. Pineri, R. Duplessix, A.M. Levelut, Small-angle scattering studies of Nafion membranes, J. Polym. Sci. Polym. Phys. Ed 19 (1) (1981) 1–11.
[17] P.C. van der Heijden, L. Rubatat, O. Diat, Orientation of drawn Nafion at molecular and mesoscopic scales, Macromolecules 37 (14) (2004) 5327–5336.
[18] M. Kim, C.J. Glinka, S.A. Grot, W.G. Grot, SANS study of the effects of water vapor sorption on the nanoscale structure of perfluorinated sulfonic acid (Nafion) membranes, Macromolecules 39 (14) (2006) 4775–4787.
[19] L. Rubatat, A.L. Rollet, G. Gebel, O. Diat, Evidence of elongated polymeric aggregates in Nafion, Macromolecules 35 (10) (2002) 4050–4055.
[20] G. Gebel, O. Diat, Neutron and X-ray scattering: suitable tools for studying ionomer membranes, Fuel Cell. 5 (2) (2005) 261–276.
[21] C.K. Knox, G.A. Voth, Probing selected morphological models of hydrated Nafion using large-scale molecular dynamics simulations, J. Phys. Chem. B 114 (9) (2010) 3205–3218.
[22] R. Herrera Alonso, L. Estevez, H. Lian, A. Kelarakis, E.P. Giannelis, Nafion-clay nanocomposite membranes: morphology and properties, Polymer 50 (11) (2009) 2402–2410.
[24] A. Kusoglu, A.Z. Weber, New insights into perfluorinated sulfonic-acid ionomers, Chem. Rev. 117 (3) (2017) 987–1104.
[25] X. Kong, K. Schmidt-Rohr, Water-polymer interfacial area in Nafion: comparison with structural models, Polymer 52 (9) (2011) 1971–1974.